Atmos. Chem. Phys., 16, 14741–14754, 2016
www.atmos-chem-phys.net/16/14741/2016/
doi:10.5194/acp-16-14741-2016

Atmospheric Chemistry and Physics
Open Access
EGU

Air–surface exchange of gaseous mercury over permafrost soil: an investigation at a high-altitude (4700 m a.s.l.) and remote site in the central Qinghai–Tibet Plateau

Zhijia Ci[1], **Fei Peng**[2], **Xian Xue**[2], **and Xiaoshan Zhang**[1]

[1]Research Center for Eco-Environmental Sciences, Chinese Academy of Sciences, Beijing, 100085, China
[2]Cold and Arid Regions Environmental and Engineering Research Institute, Chinese Academy of Sciences, Lanzhou, 730000, China

Correspondence to: Zhijia Ci (zjci@rcees.ac.cn)

Received: 17 June 2016 – Published in Atmos. Chem. Phys. Discuss.: 19 July 2016
Revised: 10 November 2016 – Accepted: 14 November 2016 – Published: 25 November 2016

Abstract. The pattern of air–surface gaseous mercury (mainly Hg(0)) exchange in the Qinghai–Tibet Plateau (QTP) may be unique because this region is characterized by low temperature, great temperature variation, intensive solar radiation, and pronounced freeze–thaw process of permafrost soils. However, the air–surface Hg(0) flux in the QTP is poorly investigated. In this study, we performed field measurements and controlled field experiments with dynamic flux chambers technique to examine the flux, temporal variation and influencing factors of air–surface Hg(0) exchange at a high-altitude (4700 m a.s.l.) and remote site in the central QTP. The results of field measurements showed that surface soils were the net emission source of Hg(0) in the entire study (2.86 $\mathrm{ng\,m^{-2}\,h^{-1}}$ or 25.05 $\mathrm{\mu g\,m^{-2}\,yr^{-1}}$). Hg(0) flux showed remarkable seasonality with net high emission in the warm campaigns (June 2014: 4.95 $\mathrm{ng\,m^{-2}\,h^{-1}}$; September 2014: 5.16 $\mathrm{ng\,m^{-2}\,h^{-1}}$; and May–June 2015: 1.95 $\mathrm{ng\,m^{-2}\,h^{-1}}$) and net low deposition in the winter campaign (December 2014: -0.62 $\mathrm{ng\,m^{-2}\,h^{-1}}$) and also showed a diurnal pattern with emission in the daytime and deposition in nighttime, especially on days without precipitation. Rainfall events on the dry soils induced a large and immediate increase in Hg(0) emission. Snowfall events did not induce the pulse of Hg(0) emission, but snowmelt resulted in the immediate increase in Hg(0) emission. Daily Hg(0) fluxes on rainy or snowy days were higher than those of days without precipitation. Controlled field experiments suggested that water addition to dry soils significantly increased Hg(0) emission both on short (minutes) and relatively long (hours) timescales, and they also showed that UV radiation was primarily attributed to Hg(0) emission in the daytime. Our findings imply that a warm climate and environmental change could facilitate Hg release from the permafrost terrestrial ecosystem in the QTP.

1 Introduction

Soils represent the largest Hg reservoirs in ecosystems and play a major role in the global Hg cycle (Selin, 2009; Agnan et al., 2016). Background soils receive Hg input from atmospheric deposition, which is mainly retained in organic-rich layers of upper soils (Schuster, 1991; Khwaja et al., 2006). Hg in soils can be reduced to Hg(0) and then emitted to the overlaying air because of its high volatility (Schlüter, 2006). Therefore, soils can serve as both sources and sinks of atmospheric Hg (Pirrone and Mason, 2009; Amos et al., 2013; Agnan et al., 2016).

In the past several decades, efforts have been made to improve the understanding of soil Hg biogeochemistry (Zhang and Lindberg, 1999; Lin et al., 2010; Schlüter, 2006; Jiskra et al., 2015). Measurements across various types of soils and climates show that air–soil Hg(0) exchange has highly spatial and temporal variation and bidirectional exchange behavior (Agnan et al., 2016, and references therein). Field measurements and laboratory experiments highlight that various factors and processes influence air–surface Hg(0) exchange, including concentrations and species of soil Hg (Gustin et al., 1999, 2002; Hintelmann et al., 2002; Bahlmann et al., 2006;

Kocman and Horvat, 2010; Eckley et al., 2011; Edwards and Howard, 2013; Mazur et al., 2015), solar radiation (Gustin et al., 2002, 2006; Moore and Carpi, 2005; Xin et al., 2007; Fu et al., 2008a; Kocman and Horvat, 2010; Park et al., 2014), precipitation (Lindberg et al., 1999; Gustin and Stamenkovic, 2005; Gabriel et al., 2011), soil temperature and moisture (Gustin et al., 1997; Gustin and Stamenkovic, 2005; Ericksen et al., 2006; Xin et al., 2007; Briggs and Gustin, 2013; Park et al., 2014; Mazur et al., 2015), soil organic matter and pH (Yang et al., 2007; Xin and Gustin, 2007; Mauclair et al., 2008), land cover (Dommergue et al., 2003; Ericksen et al., 2005; Cobbett et al., 2007; Gabriel and Williamson, 2008; Zhu et al., 2011; Durnford et al., 2012a, b; Toyota et al., 2014a, b), atmospheric Hg(0) concentrations and other chemical compositions (Engle et al., 2004; Xin and Gustin, 2007; Fu et al., 2008a), biological activity (Choi and Holsen, 2009), and atmospheric turbulence (Gustin et al., 1997; Poissant et al. 1999). Existing studies on Hg(0) dynamics at the air–surface interface are mainly performed in temperate regions (Agnan et al., 2016, and references therein). The seasonal frozen soils and permafrost widely distribute, accounting for almost 70 % of terrestrial area of Earth (NSIDC, 2016). However, the knowledge of air–surface Hg(0) dynamics in cold regions is limited (Cobbett et al., 2007; Durnford and Dastoor, 2011). Most current parameters of air–soil Hg(0) exchange applied in Hg biogeochemical models are mainly derived from temperate regions of North America and Europe (Zhu et al., 2016).

The Qinghai–Tibet Plateau (QTP) is located in western China with an area of 2.5 million km^2 and mean altitude of >4000 m. Due to the high altitude and subsequent low temperature, a significant portion (~ 1.5 million km^{-2}) of the QTP is underlain by permafrost (Kang et al., 2010). Because of the harsh natural environment, limited research resources and difficulty of access and sampling logistics, studies on Hg biogeochemistry in the QTP are limited. The role of the QTP in the regional and global Hg biogeochemical cycle is poorly understood (Ci et al., 2012; Agnan et al., 2016). At present, Hg studies in the QTP have mainly focused on investigations of Hg concentration, speciation and distribution in environmental samples, such as air (Fu et al., 2008b; 2012; Yin et al., 2015), snow and glaciers (Loewen et al., 2007; Wang et al., 2008; Zhang et al., 2012; Huang et al., 2012), and rain water (Huang et al., 2013). The knowledge of Hg(0) dynamics at the air–surface interface in the QTP is extremely poor. The unique climatic conditions, land cover and soil properties suggest the need for the specific air–soil Hg(0) flux data and a mechanism representative of the environmental setting in the QTP to better constrain global natural sources inventories (Ci et al., 2012; Agnan et al., 2016).

It is noted that many studies addressed that precipitation greatly influences air–surface Hg(0) flux over different timescales (Lindberg et al., 1999). However, previous studies have mainly focused on the effect of rainfall/watering on air–soil Hg(0) flux (Lindberg et al., 1999; Johnson et al., 2003; Gustin and Stamenkovic, 2005; Song and Van Heyst, 2005; Corbett-Hains et al., 2012) or the fate and transport of Hg(0) at the air–snow interface (Lalonde et al., 2001, 2003; Ferrari et al., 2005; Dommergue et al., 2003, 2007; Faïn et al., 2007; Bartels-Rausch et al., 2008; Brooks et al., 2008; Steen et al., 2009; Durnford et al., 2012a, b; Mann et al., 2015). Field studies on the effect of snowmelt on Hg(0) flux are very limited (Cobbett et al., 2007).

In this study, we the applied dynamic flux chamber (DFC) technique to investigate the flux, temporal variation and influencing factors of air–surface Hg(0) exchange at a representative research station in the central QTP. At the same time, controlled field experiments were performed to explore the effect of rainfall and different wavebands of solar radiation on air–soil Hg(0) flux. Combining the results of this study and other knowledge, we discuss the effect of future climatic and environmental change on air–surface Hg(0) dynamics in the QTP.

2 Methods

2.1 Study site

The study was performed at the Beiluhe Permafrost Engineering and Environmental Research Station affiliated with the Cold and Arid Regions Environmental and Engineering Research Institute, Chinese Academy of Sciences (CAREER–CAS). The elevation of the Beiluhe region is about 4700 to 4800 m a.s.l. The station (34°49′45″ N, 92°56′06″ E) lies over the continuous permafrost zone in the central QTP (Fig. 1). The terrain is undulating with sparse vegetation and surface fine sands or gravels. The thickness of the active layer and permafrost around the station is 2.0–3.2 and 60–200 m, respectively; the active layer begins to freeze in September and thaw in May (Peng et al., 2015a). The Beiluhe region experiences a continental climate with cold winter (up to −30 °C) and warm summer (up to 25 °C). The magnitude of daily air temperature is up to 30 °C, and the annual mean surface air temperature is about −2 to −3 °C (Peng et al., 2015a). The solar radiation is high and characterized by intense UV radiation (Wei et al., 2006). The mean annual precipitation is about 300 mm, and the annual potential evapotranspiration (~ 1300 mm) greatly exceeds the precipitation (Peng et al., 2015a). As it is a remote region, there is no direct human activity to influence the local Hg cycle.

The precipitation at the Beiluhe station mainly occurs during May to October under the influence of the southern Asian monsoon (Peng et al., 2015a). Due to the high-altitude location of the Beiluhe station, snow events commonly occur in May to June and late September to October. Because of intensive solar radiation and surface temperature, the snow melts or sublimates on a short timescale (1–100 h), i.e., little/no snow accumulation occurs for a long time (>3 day). Therefore, the Beiluhe region provides an

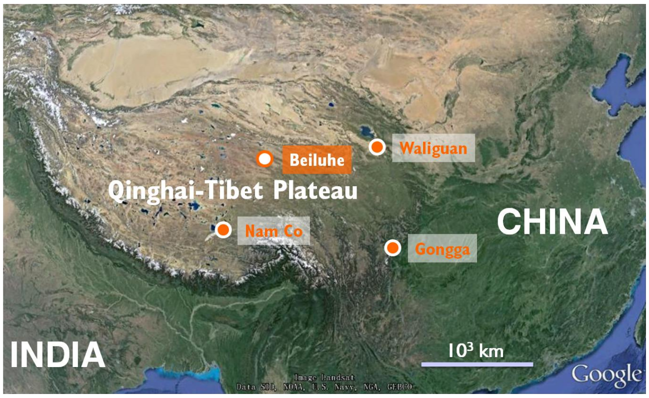

Figure 1. Locations of the Beiluhe station (4760 m a.s.l., this study), Mt. Waliguan (3816 m a.s.l., Fu et al., 2012), Mt. Gongga (1640 m a.s.l.; Fu et al., 2008b) and Nam Co (4730 m a.s.l.; Yin et al., 2015) where atmospheric Hg was determined.

unique opportunity to investigate the different effects of rain, snow, and snowmelt on the air–surface Hg(0) flux over different timescales.

2.2 Measurement of air–surface Hg(0) flux

The dynamic flux chamber (DFC) technique was widely used to investigate Hg(0) flux between the air and surface because it is inexpensive, portable, easy to set up and operate (e.g., Kim and Lindberg, 1995; Carpi and Lindberg, 1998; Gustin et al., 2006; Wang et al., 2006; Dommergue et al., 2007; Fu et al., 2008a; Kocman and Horvat, 2010; Edwards and Howard, 2013). Air–surface Hg(0) flux obtained by DFC technique was calculated using Eq. (1),

$$F = Q\frac{C_0 - C_i}{A}, \tag{1}$$

where F is the Hg(0) flux (ng m^{-2} h^{-1}), Q is the flushing flow through the chamber (m^3 h^{-1}), A is the footprint of the chamber (m^2), C_0 and C_i (ng m^{-3}) are air Hg(0) concentrations at outlet and inlet of the chamber, respectively. Positive flux values indicate Hg(0) emission from the surface into the air; negative flux values represent Hg(0) deposition to the surface from the air.

In this study, quartz chambers were constructed for measuring Hg(0) flux and exploring the effect of different rainfall depths and radiation condition on the Hg(0) flux. Quartz glass has many advantages as a construction material used in chambers for determining Hg(0) flux in background soils. First, it has high transmittance of the full spectrum of solar radiation, especially the UV waveband (Fig. S1 in Supplement). Therefore, a quartz chamber is suitable for determining the more “actual” Hg(0) flux because the short wavelength of solar radiation has been found to have an important effect on Hg(0) dynamics at the air–soil interface (Moore and Carpi, 2005; Bahlmann et al., 2006). Second, it has low potential for Hg(0) adsorption and is easy to clean by heating to remove Hg bonding on the surface (Ci et al., 2016a). The low systematic blank of quartz chamber is critical for investigating Hg(0) flux over background soils (Carpi and Lindberg, 1998).

Our semi-cylindrical quartz chamber was 8 cm high and 24 cm long with a footprint of 0.0384 m^{-2} (0.16 m × 0.24 m) and an internal volume of 2.41 L, which is similar to previous studies (Eckley et al., 2010, and references therein). The chamber had nine inlets (8 mm in diameter) and three outlets which were on the two opposite sides of the chamber. The inlet sampling tube was placed near the ground surface (3 cm above the surface) directly near the inlet of the chamber. A flushing ambient air was drawn by vacuum pump (KNF Inc., Germany) with 3.0 L min^{-1} (0.18 m^3 h^{-1}) through the chamber.

Due to the harsh environmental conditions and the unstable power supply, use of the commercial automatic Hg analyzer (such as Tekran 2537) to conduct field measurements of Hg(0) flux is challenging in the Beiluhe station. Therefore, air Hg(0) concentrations in the both inlet and outlet of the chamber were monitored manually by a gold trap simultaneously at 2–3 h intervals (Ci et al., 2016b). The air was pumped through gold trap using air pump (KNF Inc., Germany) with 0.50 L min^{-1} (0.03 m^3 h^{-1}). Hg(0) collected on gold traps was quantified on site by a cold vapor atomic fluorescence spectrophotometer (CVAFS, model III, Brooks Rand, USA) using two-stage gold amalgamation method (Fitzgerald and Gill, 1979; Ci et al., 2011, 2016a). Gold trap efficiencies were determined in laboratory (Hg(0) concentration: 3.2 to 13.4 ng m^{-3}) and field (Hg(0) concentration: ∼ 1 to 2 to 9.4 ng m^{-3}), and multiple measurements using gold traps in series showed no breakthrough at the sample flow rate of 0.50 L min^{-1} for 5 h. The method detection limit was 0.03 ng m^{-3} and precision was 3 ± 2 %.

The turnover time obtained from this protocol was 0.68 min, which is similar to previous studies (Eckley et al., 2010, and references therein). The flow rates of air both the inlet and outlet of the chamber were adjusted by a needle valve and controlled by a rotameter. Prior to the measurement, the rotameters were calibrated by a mass flow meter and a volumetric gas meter. The accuracy of flow rate was ±3 %. The sampling control system was installed in the tent near the soil plot (< 2 m).

In this study, a bare soil plot of 2 m × 2 m was chosen and separated into four subplots (1 m × 1 m, labeled as Subplot A to D) to measure Hg(0) flux and further to investigate the effects of different wavelengths of solar radiation on the Hg(0) exchange. The soil parent materials in the study site is mainly composed of sand (> 99 %) (Peng et al., 2015a). Geologic unit of this soil plot is representative of major lithologic units of the Beiluhe region. The study was conducted in four campaigns (June, September, and December 2014 and May–June 2015), covering typical intra-annual meteorological condition in the study region. It is well known

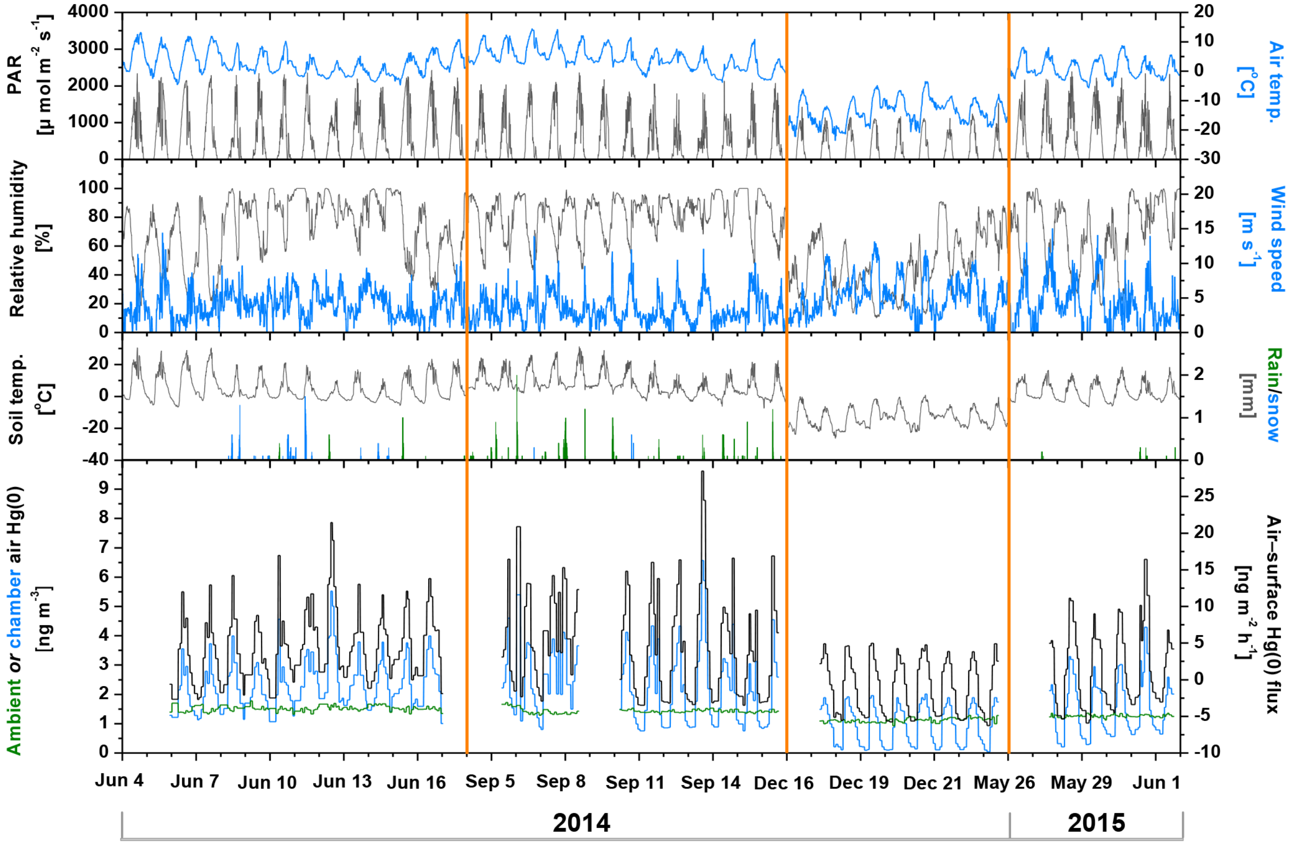

Figure 2. Temporal variation in environmental variables, air Hg(0) concentrations inside and outside of the chamber, and air–surface Hg(0) flux at the Beiluhe station in the central QTP during four campaigns in 2014–2015.

that the application of the chamber isolates the soil surface from air turbulence and rain, dew, frost or snow, altering many environmental parameters that influence Hg(0) production/consumption and deposition/emission at the air–soil interface (Sommar et al., 2012, and references therein). In the Beiluhe region, rain, dew, frost or snow commonly occurs on a short timescale (10^1–10^2 min) because of the high-altitude location and great variation in temperature and unstable weather conditions. To minimize the effect of great variation in soil surface condition on Hg(0) flux measurements, when only measuring Hg(0) flux, we used the same chamber to measure Hg(0) flux in four subplots (Subplot A to D) in turn. For the rainy and snowy days, if possible, the chamber was moved to next subplot generally after the rain or snow because studies confirmed the significant influence of precipitation on Hg(0) flux on a short timescale (Lindberg et al., 1999; Gustin and Stamenkovic, 2005; Johnson et al., 2003; Song and Van Heyst, 2005; Lalonde et al., 2001, 2003; Dommergue et al., 2003, 2007, 2012; Faïn et al., 2007; Bartels-Rausch et al., 2008; Brooks et al., 2008; Mann et al., 2014, 2015). For the days without precipitation, the chamber was moved to the next subplot before sunrise to capture the effect of frost or dew on air–surface Hg(0) flux in the light.

In this study, all materials in contact with Hg(0) were quartz, Teflon or borosilicate glass. The chambers and tubing were rigorously acid-washed (Ci et al., 2016a). The quartz chambers were heated to 650 °C for 2 h prior the measurement to further remove all Hg (Ci et al., 2016a). System blanks of the four chamber systems were systemically inspected on site by placing acid-cleaned Teflon filter beneath the chamber and routinely inspected before and after the measurements under field conditions. The overall blank results were taken as the average of all chamber blanks for each particular day or from the entire period if continuous monitoring was conducted. The blank values of the four chambers were found to be very low (mean ± SD: -0.02 ± 0.03 ng m^{-2} h^{-1}; range: -0.20–0.07 ng m^{-2} h^{-1}) and were not significantly different ($p > 0.05$) throughout the entire study. We also found that the mean blank values were not significantly different ($p > 0.05$) from zero and were insignificant compared to the measured Hg(0) fluxes (see below); thus, Hg(0) flux data were not blank-corrected in this study.

2.3 Controlled field experiments

2.3.1 Water addition

To explore the effect of water addition in detail, we chose another similar soil plot with homogeneous soil properties to conduct controlled field experiments in order to investigate the effect of different rainfall depths on Hg(0) flux over different timescales (from minutes to hours). The controlled experiments were performed during the May–June 2015 campaign since this period had high surface temperature and low precipitation (Fig. 2). In the Beiluhe station, hourly rainfall depth rarely exceeds 15 mm (Peng et al., 2015a). Therefore, we designed four different treatments of rainfall depth (0, 1, 5, and 15 mm). The water addition to the dry soils commenced at night (01:40 LT) on 30 May 2015 to exclude the effect of photochemical process in the first hours of experiments. We added the Milli-Q water (Hg concentration $<0.2\,\mathrm{ng\,L^{-1}}$) to the inside and outside of the chamber with a pre-cleaned plastic syringe within 10 min to simulate the three different rain depths. Four chambers were used to simultaneously measure Hg(0) flux over these four treatments for 22 h (from 01:00 to 23:00 LT) with the same protocol described in the Methods section. Hg(0) flux was measured with 20 min intervals in the first hours (from 01:00 to 04:20 LT) of the experiments to investigate the temporal variation in Hg(0) flux in the short timescale, and with 1 h intervals for the rest period of the experiments.

2.3.2 Different wavebands of solar radiation

The QTP is characterized by high solar radiation with intense UV radiation. We performed the controlled experiment to quantify the role of different wavebands of solar radiation (UVB, UVA and visible light) in air–soil Hg(0) flux. Four chambers with different exposure treatments were used to measure Hg(0) flux simultaneously in the daytime. Chamber A was used to measure the Hg(0) flux in the natural light. Chamber B and chamber C were covered with UVB and UV filters to remove the corresponding wavebands from the natural light. Chamber D covered with foil was used to measure Hg(0) flux in the dark. The experiments were performed in 4 days without precipitation (21–22 December 2014 and 29–30 May 2015) to exclude the effect of precipitation. Hg(0) flux triggered by UVB, UVA and visible light was equal to difference of flux between chamber A and chamber B, between chamber B and chamber C, and between chamber C and chamber D, respectively. The transmittance of UVB filter and UV filter was shown in Fig. S1.

2.4 Determination of soil Hg

Surface soil samples (0–2 cm) were collected from four soil subplots during the June 2014 campaign. Soil samples were freeze-dried and homogenized for total Hg determination using a Milestone DMA direct Hg analyzer (detection limit: 0.01 ng Hg or $0.15\,\mathrm{\mu g\,kg^{-1}}$) following EPA Method 7473 (Briggs and Gustin, 2013), and the analytical accuracy was 3 %.

2.5 Measurements of environmental variables

A meteorological station that located 60 m from the soil plot was used to collect the following environmental variables: air temperature (°C), relative humidity (%), wind speed ($\mathrm{m\,s^{-1}}$), precipitation (mm), photosynthetically active radiation (PAR, $\mathrm{\mu mol\,m^{-2}\,s^{-1}}$), and surface soil temperature (°C). The surface soil temperature was monitored by an ASI-111 precision infrared radiometer (Campbell Scientific Inc., USA). This sensor was installed on a bar 0.8 m above the soil surface and provided a non-contact measurement of the surface temperature. We also measured the soil temperature at 1.0 cm soil depth on the inside of the chamber, and no significant difference was found between the soil temperature in the outside and inside of the chamber. Details on the measurements of environmental variables are given in Peng et al. (2015a). The thickness of snowpack was measured manually.

3 Results and discussion

3.1 Soil Hg

Soil Hg concentrations of four subplots varied from 13.11 ± 0.51 to $12.83 \pm 0.81\,\mathrm{\mu g\,kg^{-1}}$, suggesting that the study region is a typical background soil for Hg. Soil Hg concentrations and air–soil Hg(0) flux of four subplots were not statistically different ($p > 0.05$), indicating the properties of the soil plot were homogeneous.

3.2 Hg(0) in ambient air

Figure 2 shows the temporal variation in air Hg(0) concentrations inside and outside of the chamber, air–surface Hg(0) flux and environmental variables during four campaigns in 2014–2015. Hg(0) concentrations of ambient air ranged from 0.93 to $1.78\,\mathrm{ng\,m^{-3}}$ with a mean of $1.36 \pm 0.17\,\mathrm{ng\,m^{-3}}$ ($n = 361$), which were slightly lower than those in typical Northern Hemisphere background regions ($\sim 1.5\,\mathrm{ng\,m^{-3}}$; Sprovieri et al., 2007; Ebinghaus et al., 2011). To our knowledge, only four measurements (including this study) have been conducted to determine atmospheric Hg over the QTP (see Fig. 1 for the locations). The gradient of atmospheric Hg(0) over the QTP was characterized by high concentrations in Mt. Gongga ($3.98 \pm 1.62\,\mathrm{ng\,m^{-3}}$; Fu et al., 2008b) and Mt. Waliguan ($1.98 \pm 0.98\,\mathrm{ng\,m^{-3}}$; Fu et al., 2012), moderate concentrations in the Beiluhe ($1.36 \pm 0.17\,\mathrm{ng\,m^{-3}}$, this study), and low concentrations in the Nam Co ($0.96 \pm 0.19\,\mathrm{ng\,m^{-3}}$; Yin et al., 2015). It seems that the sampling station with relatively long distance from the source region of atmospheric Hg(0) (i.e., central China;

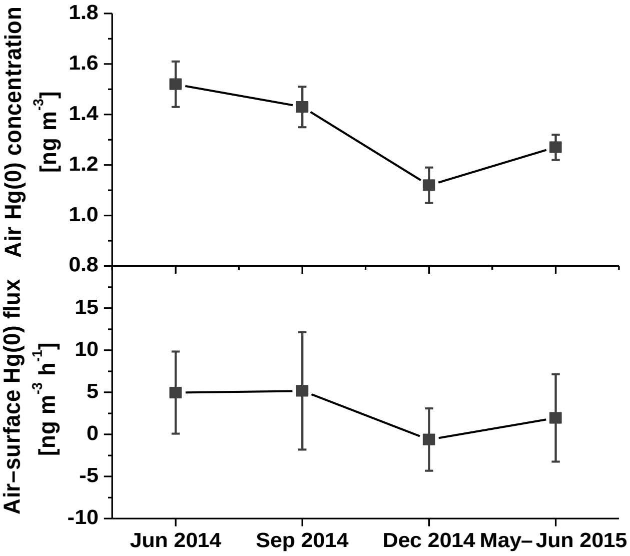

Figure 3. Seasonal variation in Hg(0) concentration in ambient air and air–surface Hg(0) flux during four campaigns at the Beiluhe station in the central QTP in 2014–2015.

Streets et al., 2005) had relatively low atmospheric Hg(0) concentrations (Fig. 1). Atmospheric Hg(0) concentrations were high in three warm campaigns and low in the winter campaign in the Beiluhe station (Fig. 3), which is consistent with Mt. Gongga (Fu et al., 2008b) and Mt. Waliguan (Fu et al., 2012).

3.3 Air–surface Hg(0) flux and influencing factors

3.3.1 Temporal variation in Hg(0) flux

The mean of air–surface Hg(0) flux in the entire study period were 2.86 $\mathrm{ng\,m^{-2}\,h^{-1}}$ (25.05 $\mathrm{\mu g\,m^{-2}\,yr^{-1}}$), indicating that surface soils were the net emission source of Hg(0). Hg(0) flux in this study is comparable to that over background soils (-10–10 $\mathrm{ng\,m^{-2}\,h^{-1}}$; Wang et al., 2006; Ericksen et al., 2006; Fu et al., 2008a) but greatly lower than those over Hg-enriched soils (10^2–10^3 $\mathrm{ng\,m^{-2}\ h^{-1}}$; Gustin et al., 1999; Wang et al., 2007; Edwards and Howard, 2013), indicating that soil Hg concentrations may be the dominant factor for controlling the magnitude of Hg(0) emission flux (Agnan et al., 2016, and references therein).

Figure 2 shows that the Hg(0) flux was highly variable. The highest Hg(0) emission fluxes of 28.46 $\mathrm{ng\,m^{-2}\,h^{-1}}$ were observed at 13:00–15:00 LT on 13 September 2014 after a rain event on dry soils. The highest Hg(0) deposition fluxes of -6.24 $\mathrm{ng\,m^{-2}\,h^{-1}}$ were observed at nighttime over the cold and dry surface soil during the December 2014 campaign (03:30–06:30 LT, 24 December 2014).

Hg(0) flux generally showed a diurnal pattern with high emission in the daytime and remarkable deposition in nighttime, especially on days without precipitation (Fig. 2). Many studies have confirmed that solar radiation is one of the most important drivers for soil Hg(0) emission (Xin and Gustin, 2007; Choi and Holsen, 2009; Kocman and Horvat, 2010); high surface temperature also facilitates Hg(0) production and subsequent emission (Park et al., 2014). Therefore, the two environmental variables jointly regulate the diurnal pattern of Hg(0) flux. An in-depth discussion on synergistic effects of solar radiation and surface temperature on Hg(0) flux is provided below. Interestingly, the diurnal pattern of Hg(0) flux of each day during the December 2014 campaign was almost identical, which may be associated with very similar weather conditions throughout the entire campaign.

Hg(0) flux showed pronounced seasonality with high emission in three warm campaigns (June 2014: 4.95 $\mathrm{ng\,m^{-2}\,h^{-1}}$; September 2014: 5.16 $\mathrm{ng\,m^{-2}\,h^{-1}}$;and May–June 2015: 1.95 $\mathrm{ng\,m^{-2}\,h^{-1}}$) and net low deposition during the winter campaign (December 2014: -0.62 $\mathrm{ng\,m^{-2}\,h^{-1}}$) (Fig. 3). Similar seasonality has been reported in many other studies (e.g., Gabriel et al., 2006). As discussed below, in warm seasons, some environmental variables, such as high solar radiation, surface temperature and precipitation, facilitate the soil Hg(0) emission.

3.3.2 Effect of precipitation (rain and snow)

Firstly, the effect of rain events on Hg(0) flux was investigated. We found that the Hg(0) emission flux increased immediately following the rainfall (Fig. 2), which is consistent with many other studies (Gustin and Stamenkovic, 2005; Johnson et al., 2003; Lindberg et al., 1999; Song and Van Heyst, 2005). Previous studies have suggested that the dramatic increases in Hg(0) emission may be attributed to the physical displacement of Hg(0) present in soil air and desorption of loosely bound Hg(0) on soil particles by the infiltrating water (Johnson et al., 2003; Gustin and Stamenkovic, 2005). Notably, Fig. 2 shows that the pulse of Hg(0) emission after the rainfall was also observed at nighttime (such as 0:00 to 01:00 LT on 4 September 2014). A similar phenomenon was also documented by our controlled experiments (see below). This indicates that the immediate increase in Hg(0) emission might not be controlled by photochemical processes but by physical processes.

Soil moisture condition may also significantly regulate Hg(0) flux over relatively long timescales (from hours to several days). Therefore, many experiments studied the effect of water addition on the magnitude and pattern of air–soil Hg(0) flux over different timescales (Johnson et al., 2003; Gustin and Stamenkovic, 2005). However, most of studies were performed in controlled laboratory or mesocosm settings under certain well-defined but not necessarily environment relevant conditions (Johnson et al., 2003; Gustin et al., 2004; Gustin and Stamenkovic, 2005; Song and Van Heyst, 2005; Kocman and Horvat, 2010; Corbett-Hains et al., 2012; Park et al., 2014). In this study, it was also challenging to reveal the effect of rainfall on Hg(0) flux over relatively long timescales

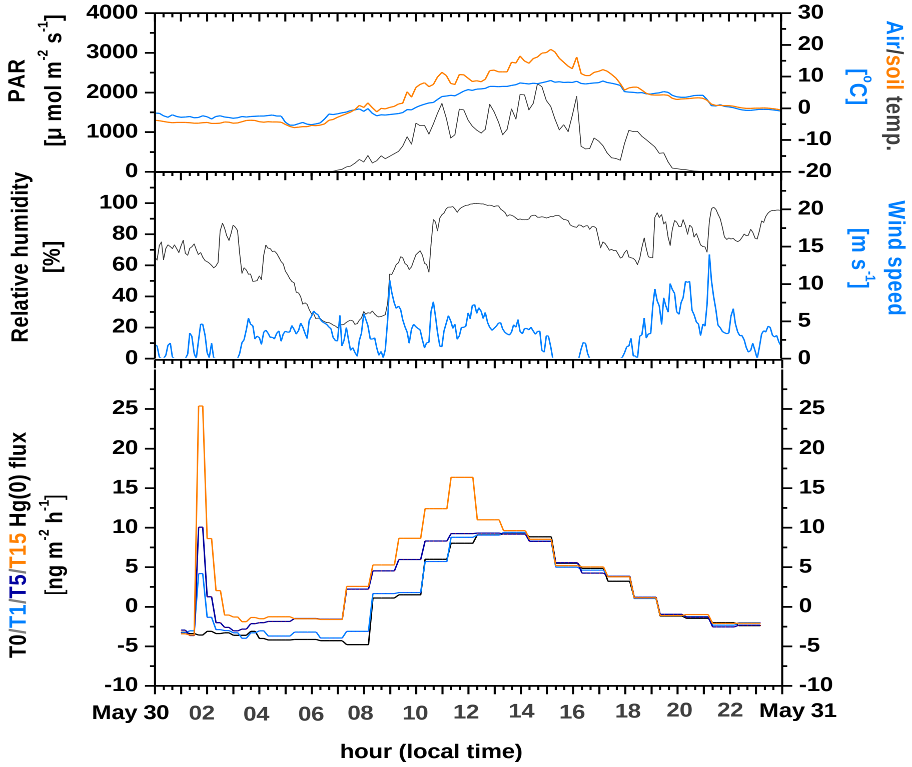

Figure 4. Temporal variation in Hg(0) flux over four soil plots with different treatment of water addition (T0: 0 mm treatment; T1: 1 mm treatment; T5: 5 mm treatment; and T15: 15 mm treatment) and the environmental variables.

via field measurement since the intermittent rain events occurred irregularly during the June 2014 and September 2014 campaign (Fig. 2). Therefore, we performed the controlled field experiments (Sect. 2.3.1) to explore the effect of different rainfall depths on Hg(0) flux over different timescales (from minutes to hours).

The high-time-resolution measurements captured the immediate and dramatic increases in Hg(0) emission flux after the watering of dry soils (Fig. 4). The baseline Hg(0) flux of the 0 mm treatment was used as the benchmark for the different rainfall depth treatments to be compared against. Obviously, the higher amount of water addition resulted in longer duration and higher accumulative flux of Hg(0) emission pulse. The duration of the Hg(0) emission pulse for the 1 mm and 5 mm treatment was <20 min (from 01:40 to 02:00 LT) and ~ 40 min (from 01:40 to 02:20 LT), respectively, which was lower than that of the 15 mm treatment (~ 80 min, from 01:40 to 03:00). The duration of Hg(0) emission for the 15 mm treatment in the daytime was also longer than that of the 1 and 5 mm treatment (Fig. 4).

As shown in Fig. 4, the cumulative flux of Hg(0) emission during the entire study period mainly included two fractions: the pulse of Hg(0) emission after the watering (i.e., emission flux by watering) and the Hg(0) emission during the daytime (i.e., emission flux by radiation). Figure 5 shows that both "emission flux by watering" and "emission flux by radiation" for the 15 mm treatment were significantly higher than those of the 1 and 5 mm treatment. As mentioned above, the dramatic increase in Hg(0) emission after the simulated rain can be explained by physical displacement of interstitial soil air by the infiltrating water. The long emission duration and large immediate emission flux for soil plot with high water addition can be explained by more water needing a longer time to percolate the soil column and displacing more soil Hg(0). Many previous studies have suggested that the magnitude of Hg(0) emission with a rainfall or stimulated rain depended on soil moisture condition – i.e., if the amounts of water received by the soils were less than needed to saturate, the soil surface showed an immediate increase in Hg(0) emission, and after the soil became saturated, Hg(0) emission from surface soil was suppressed (Klusman and Webster, 1981; Lindberg et al., 1999; Johnson et al., 2003; Gustin and Stamenkovic, 2005). In this study, the pulse of Hg(0) emission flux for the 15 mm treatment was significantly higher than that of the 5 and 1 mm treatment (Fig. 5). The field water capacity and bulk density of soil in the Beiluhe region is about 28 % and 1 g cm^{-3} (Peng et al., 2015b), indicating that the 5 mm treatment may cause the upper soil to saturate on a short timescale since the duration of water addition was short (<10 min). However, the pulse of Hg(0) emission for the 15 mm treatment was significantly higher than that of the 5 mm treatment. The surface soils with high sand con-

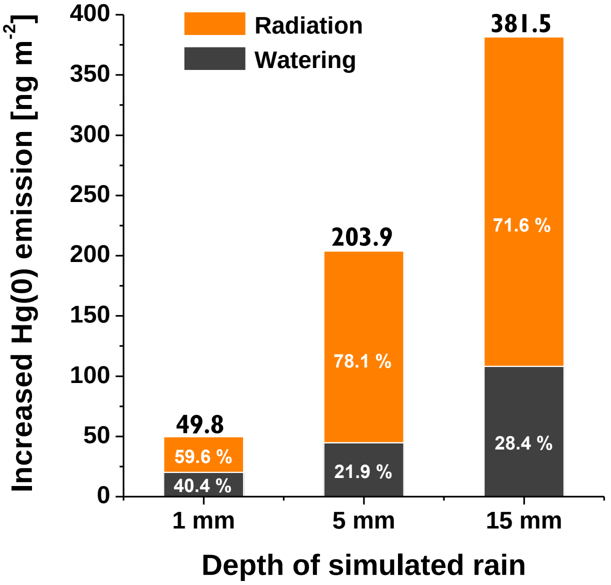

Figure 5. Increased Hg(0) emission for three different treatments (1, 5 and 15 mm addition of water) compared with the 0 mm treatment during the controlled experiment on 30 May 2015.

tent in the Beiluhe region have a high rate of water infiltration and subsequently great infiltration depth. This process potentially increases the displacement of soil Hg(0) and facilitates Hg(0) emission, as mentioned above. Therefore, under the field conditions, the duration and flux of pulse Hg(0) emission following water addition depends not only on the amount of water received and soil moisture condition but also soil texture and soil water dynamics.

The water addition also increased the Hg(0) emission in the daytime, showing more water added, longer duration of Hg(0) emission, and more Hg(0) emitted (Figs. 4 and 5). After the surface soil was visibly dry, Hg(0) flux over soil plots with water addition had no significant difference from that of the soil plot without water addition (i.e., 0 mm treatment). This result is consistent with many other controlled studies. For example, Johnson et al. (2003) and Gustin and Stamenkovic (2005) found that once the soil water content became less than saturated, Hg(0) emission flux would be significantly enhanced, especially during the daytime, and once sufficient drying occurred, the magnitude of Hg(0) emission flux tended to gradually decrease. Investigators have suggested that as the water evaporates and soil dries, capillary action drives the upward movement of water and chemicals (including Hg components) and recharges the Hg pool in surface soils (i.e., the “wick effect”) and subsequently favors the Hg(0) production and emission via photochemical processes in the light (Gustin and Stamenkovic, 2005). In our study, even for the wettest soil plot (i.e., 15 mm treatment), the surface soils were visually unsaturated in the daytime because of the low water retention, high infiltration rate of local soils and intensive solar radiation. Therefore, the pattern of Hg(0) emission for soil plots with high water addition is comparable to those of the above-mentioned studies.

Secondly, the effect of snow events on Hg(0) flux were investigated. One of the most significant differences between the rainfall and snowfall on the effect of Hg(0) exchange was that the snowfall did not induce the remarkable pulse of Hg(0) emission. For example, at 10:10 LT on 11 June 2014, a heavy snowfall event occurred, which continued until 11:20 LT. The highest thickness of the snowpack reached ∼ 12 cm. However, no remarkable pulse of Hg(0) emission was observed during the snowfall. Instead, the Hg(0) dynamics at the air–snow interface showed a clear diurnal pattern with high emission in the daytime and deposition or emission, albeit rather small, in the nighttime. This finding is consistent with previous studies on the air–snow interface (Cobbett et al., 2007). It can be seen that the pattern of Hg(0) dynamics at the air–snow interface was similar with that at the air–soil interface, indicating that Hg(0) emission from surface snow was also mainly regulated by photochemical processes (Ferrari et al., 2005; Dommergue et al., 2003, 2007). However, it is well known that the snowpack is a porous matrix, and gases are subjected to diffusion in the snowpack. Therefore, our measurements of Hg(0) flux at the air–snow interface did not exclude the effect of Hg(0) dynamics at the soil–snow interface, especially the low thickness (< 12 cm) of snowpack in the study.

We found that the snow melting led to the remarkable peak of Hg(0) emission. For example, during the sunrise of 12 June 2014, a precipitation event with rain and snow caused the snowpack (12 cm) to melt suddenly and completely (i.e., bare soil with no surface snow) and a pulse of Hg(0) emission ($\sim 8\,\mathrm{ng\,m^{-2}\,h^{-1}}$) was observed, which was the largest Hg(0) emission flux during the June 2014 campaign. We supposed that the great increase in Hg(0) emission by snowmelt in this study was consistent with the effect of rainfall, i.e., the displacement of soil Hg(0) during the snowmelt permeation of the soil column resulted in the dramatic increase in Hg(0) emission. At present, the study on the effect of snowpack melting on Hg(0) emission is limited. Cobbett et al. (2007) also found the remarkable increase in Hg(0) emission in Canadian Arctic during the snowmelt, although the Hg(0) flux was relatively small.

Finally, the effect of precipitation (including rain and snow) on daily Hg(0) flux was investigated. The above-mentioned results and discussion suggest that the precipitation has great potential to facilitate soil Hg(0) emission over different timescales via physical, chemical and biological processes. The main processes include the displacement of soil Hg(0) by water, the “wick effect” to increase the photoreducible Hg(II) pool in surface soils, and the increased soil moisture to promote the biotic and abiotic reduction of Hg(II). Another well-documented process is that the atmospheric wet deposition of Hg will increase the Hg pool in surface soils and the newly deposited Hg is very active in reducing to Hg(0) (Hintelmann et al., 2002), although our study

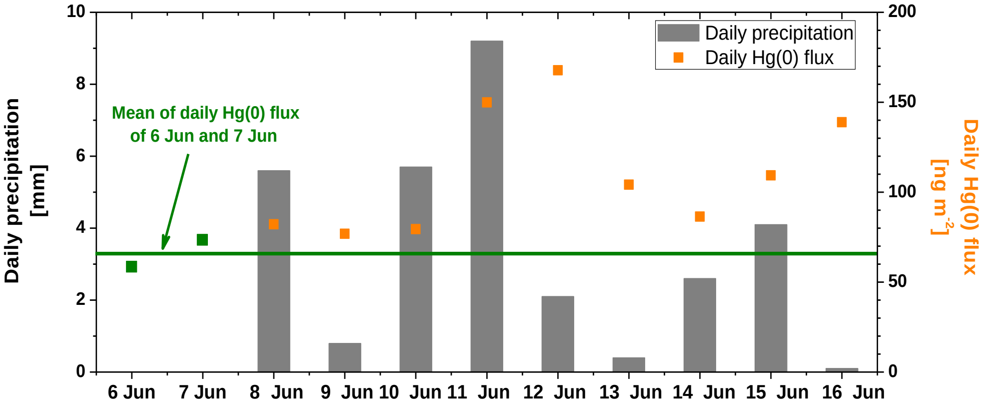

Figure 6. Daily Hg(0) flux and daily precipitation in the June 2014 campaign.

did not focus on this issue. During the June 2014 campaign, no precipitation occurred in the first 2 days (6–7 June 2014), but the rest of the days were rainy or snowy days (Fig. 2). We attempted to use the daily Hg(0) flux of the two sunny days as the benchmark to compare with those of rainy or snowy days in order to investigate the effect of precipitation on the Hg(0) flux over the timescale of one day. Figure 6 shows that the daily Hg(0) flux for rainy/snowy days was higher (ranging from 16 to 154 %) than the mean of the two sunny days. The result indicates that the precipitation increased soil Hg(0) emission on the timescale of 1 day, although the low solar radiation and temperature on rainy/snowy days would potentially decrease soil Hg(0) emission, as mentioned above.

3.3.3 Effect of solar radiation and soil temperature

Almost all laboratory experiments and field measurements, including this study, show that the high solar radiation and elevated soil temperature synergistically facilitate the soil Hg(0) emission (Edwards and Howard, 2013; Park et al., 2014). The following hypotheses have been proposed to explain the role of solar radiation and temperature in promoting soil Hg(0) emission: (1) solar radiation promotes the photoreduction of Hg(II) in surface soils to form Hg(0) on a short timescale, (2) solar radiation and high soil temperature reduce the apparent activation energy of Hg(0) desorption and increase Hg(0) emission from surface soils, and (3) the high soil temperature favors the Hg(0) production in soil column by biotic and abiotic processes (Carpi and Lindberg, 1998; Gustin et al., 2002).

Many studies used the Arrhenius equation (Eq. 2) to quantitatively investigate the relationship between soil temperature and Hg(0) flux.

$$F = \mathrm{A}e^{-E_\mathrm{a}/RT} \text{ or } \ln(F) = \ln(A) - \frac{E_\mathrm{a}}{RT}, \qquad (2)$$

where F is the Hg(0) flux ($\mathrm{ng\,m^{-2}\,h^{-1}}$), R is the gas constant, T is the soil temperature (K), A is the pre-exponential factor, and E_a is the apparent activation energy. A plot of $\ln(F)$ vs. $1/T$ obtains a straight line with an intercept equal to the log of the A, and the slop equal to $-E_\mathrm{a}/R$. Theoretically, the concept of the apparent E_a refers to the thermally controlled reaction. Therefore, Hg(0) flux induced by light and precipitation should be excluded from the correlation analysis. However, in many previous studies, especially for the field measurements, the bulk Hg(0) flux in the light was generally used to explore the contribution of solar radiation or temperature to Hg(0) flux and did not isolate the respective effect of the two factors (Fu et al., 2008a). This will systematically overestimate or underestimate the contribution of solar radiation and temperature on soil Hg(0) emission depending on the source or sink of soil for Hg(0) in the dark. Only in some controlled experiments were the separated data used to explore the respective role of radiation and temperature in soil Hg(0) emission (e.g., Kocman and Horvat, 2010).

In this study, for determining the respective contributions of solar radiation and temperature to the Hg(0) flux, in addition to Hg(0) flux being measured in natural light, Hg(0) flux in the dark was also measured simultaneously with a foil-covered chamber. The temperature-corrected Hg(0) flux (i.e., bulk Hg(0) flux in the light minus Hg(0) flux in the dark) in the daytime ($\mathrm{PAR} > 0$) was considered to be the contribution of the solar radiation. As mentioned above, the effect of precipitation should be excluded from the data set; therefore, we only collected Hg(0) flux data on days without precipitation during the December 2014 and May–June 2015 campaign.

Figure 7 displays the temporal variation in bulk Hg(0) flux in the light, Hg(0) flux in the dark, net Hg(0) flux in the light (i.e., bulk Hg(0) flux in the light – Hg(0) flux in the dark) and the environmental variables. Clearly, changes in solar radiation had a greater influence on soil Hg(0) flux than did changes in soil temperature. The data showed that the soil served as a Hg(0) sink during all study days in the December 2014 campaign in the dark with high deposition flux in low soil temperature and low deposition flux in high soil temperature. During study days of the May–June 2015 campaign,

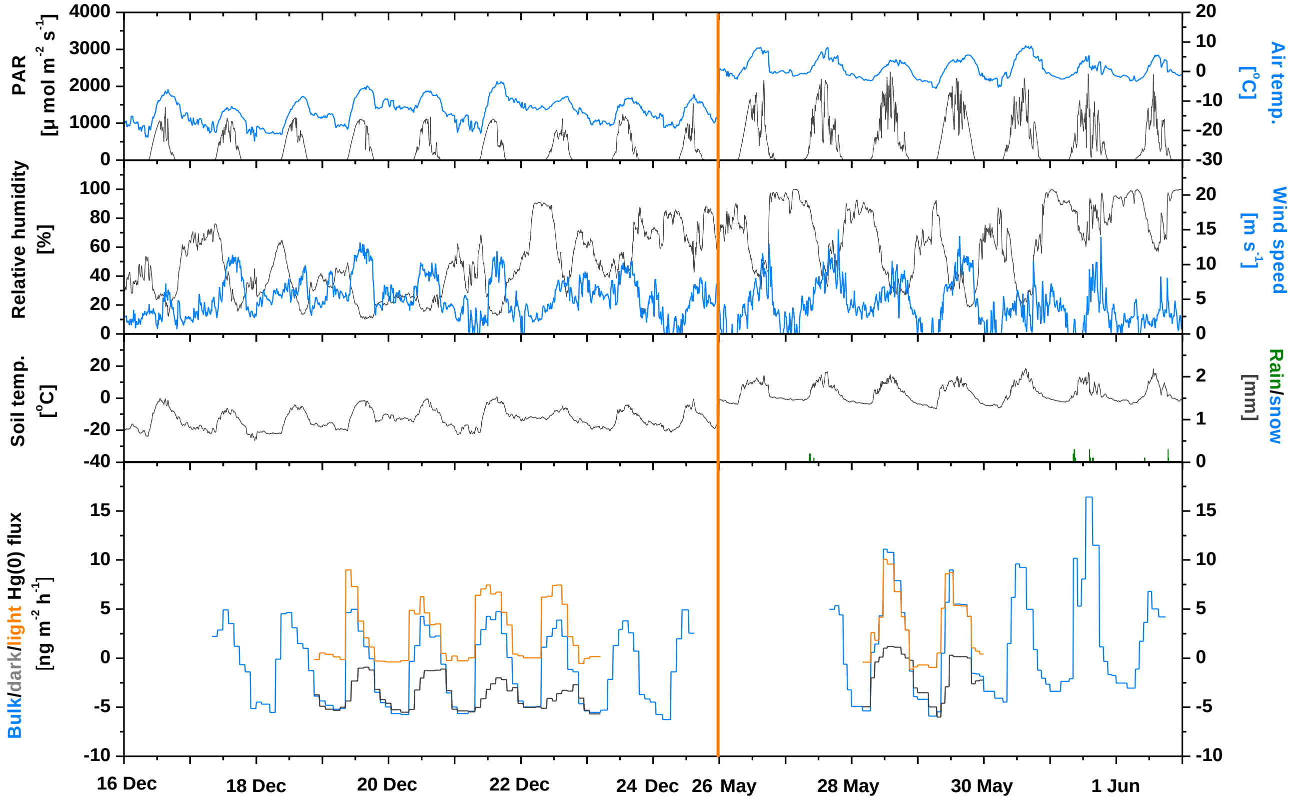

Figure 7. Temporal variation in bulk Hg(0) flux in the light, Hg(0) flux in the dark, and net Hg(0) flux in the light (bulk Hg(0) flux in the light–Hg(0) flux in the dark) in six study days without precipitation during the December 2014 campaign and May–June 2015 campaign.

the soils served as a very low Hg(0) source at midday with relatively high soil temperature. This finding is consistent with many studies in background soils (Ericksen et al., 2006; Gustin et al., 2006; Fu et al., 2008a; Edwards and Howard, 2013). It indicates that the soil temperature plays an important role in Hg(0) dynamics at the air–soil interface, i.e., low soil temperature favors absorbing Hg(0) or reducing Hg(0) emission (e.g., Park et al., 2014, and references therein).

After the temperature was corrected, except for at midday on study days during the May–June campaign, the net Hg(0) flux in the light was higher than the bulk Hg(0) flux. A positive linear correlation was found between cumulative PAR and cumulative Hg(0) flux in the daytime, although cumulative PAR only explained ∼ 28 % of variation in cumulative Hg(0) flux in the daytime (Fig. S2).

We used the Hg(0) emission data set in the dark to calculate the E_a using the Arrhenius equation. Since the soils in the dark were the sink of atmospheric Hg(0) in most of the study period, only a limited data set ($n = 9$) can be used (Fig. S3). The E_a/R for Hg(0) emission from our remote soils with extremely low Hg concentrations (∼ 12 μg kg^{-1}) was 30.40. Table S1 in Supplement lists the E_a/R for different soils with large variation in soil Hg concentrations, including this study, and shows that the E_a/R of Hg(0) emission from soils with low Hg concentrations was higher than that of soils with high Hg concentrations and significantly lower than that of the theoretical value (7.31) of elemental Hg. The result indicates that surface soils with high Hg concentrations has great potential to emit Hg(0). This trend is consistent with the laboratory study of Bahlmann et al. (2006), although the availability of Hg in soils also significantly regulates Hg(0) emission (Bahlmann et al., 2006; Kocman and Horvat, 2010).

Figure 8 shows that UV radiation was the dominant waveband of solar radiation for Hg(0) emission in the daytime, contributing > 80 % of Hg(0) emission in the light, and the contribution of UVB radiation accounted for > 50 % in all study days. This finding is consistent with previous laboratory studies (Moore and Carpi, 2005; Bahlmann et al., 2006; Xin et al., 2007).

4 Conclusions and implications

In this study, we measured the Hg(0) flux between the air and surface permafrost soil in the QTP. We also performed controlled field experiments to explore the effect of precipitation and different wavebands of solar radiation on the air–soil Hg(0) exchange. The results showed that the environmental conditions, including solar radiation, soil temperature and

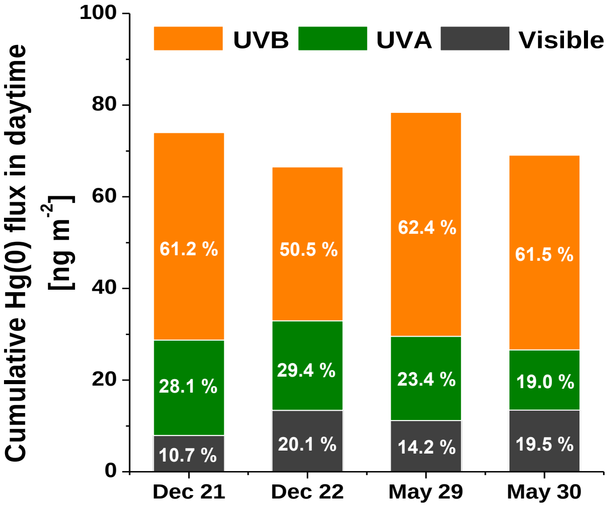

Figure 8. Cumulative Hg(0) emission flux in the daytime triggered by UVB, UVA and visible light in four study days during the December 2014 campaign and May–June 2015 campaign.

precipitation, greatly influenced the Hg(0) exchange between air and surface.

This study and other field measurements and laboratory experiments have clarified that the fate and transport of soil Hg is very sensitive to the environmental variables (Krabbenhoft and Sunderland, 2013). Therefore, our results have several important implications to the Hg biogeochemical cycle in the soils of the QTP under the rapid climate warming and environmental change. Firstly, the increased surface temperature in the QTP will potentially promote the remobilization of soil Hg. Field measurements and a modeling study have revealed that the surface temperature in the QTP is increasing, and the warming trend exceeds those for the Northern Hemisphere and the same latitudinal zone (Kang et al., 2010). Secondly, the increased UV radiation in the QTP may enhance Hg(0) emission from surface soils. UV radiation reaching the surface of the QTP is estimated to increase because of the decrease of stratospheric O_3 (Zhou et al., 2013). Our result and many of the above-mentioned studies show that UV radiation plays the primary role in promoting the surface Hg(0) emission in the daytime. Thirdly, the temporal–spatial pattern of precipitation in the QTP is also changing (Kang et al., 2010), which potentially alters the flux and temporal–spatial pattern of air–soil Hg(0) exchange in this region because of the importance of precipitation on the Hg(0) exchange. However, this study was just the beginning to explore the effect of climate change on the terrestrial Hg cycle in the QTP. More studies are needed in the future.

5 Data availability

The data are available on request from the first author.

The Supplement related to this article is available online at doi:10.5194/acp-16-14741-2016-supplement.

Acknowledgements. The study was financially supported by the National Key Basic Research Program of China (no. 2013CB430002), the National Natural Science Foundation of China (no. 41573117, 41371461, 41203068), and the Young Scientists Fund of the Research Center for Eco-Environmental Sciences, Chinese Academy of Sciences (no. RCEES-QN-20130048F). We thank the staff of the Beiluhe Permafrost Engineering and Environmental Research Station affiliated with the Cold and Arid Regions Environmental and Engineering Research Institute, Chinese Academy of Sciences (CAREER–CAS), for their assistance.

Edited by: R. Ebinghaus
Reviewed by: three anonymous referees

References

Agnan, Y., Le Dantec, T., Moore, C. W., Edwards, G. C., and Obrist, D.: New constraints on terrestrial surface–atmosphere fluxes of gaseous elemental mercury using a global database, Environ. Sci. Technol., 50, 507–524, 2016.

Amos, H. M., Jacob, D. J., Streets, D. G., and Sunderland, E. M.: Legacy impacts of all-time anthropogenic emissions on the global mercury cycle, Global Biogeochem. Cy., 27, 410–421, 2013.

Bahlmann, E., Ebinghaus, R., and Ruck, W.: Development and application of a laboratory flux measurement system (LFMS) for the investigation of the kinetics of mercury emissions from soils, J. Environ. Manage., 81, 114–125, 2006.

Bartels-Rausch, T., Huthwelker, T., Jöri, M., Gäggeler, H. W., and Ammann, M.: Interaction of gaseous elemental mercury with snow surfaces: laboratory investigation, Environ. Res. Lett., 3, 52–55, 2008.

Briggs, C. and Gustin, M. S.: Building upon the conceptual model for soil mercury flux: evidence of a link between moisture evaporation and Hg evasion, Water Air Soil Pollut., 224, 1–13, 2013.

Brooks, S., Arimoto, R., Lindberg, S., and Southworth, G.: Antarctic polar plateau snow surface conversion of deposited oxidized mercury to gaseous elemental mercury with fractional long-term burial, Atmos. Environ., 42, 2877–2884, 2008.

Carpi, A., and Lindberg, S. E.: Application of a Teflon™ dynamic flux chamber for quantifying soil mercury flux: tests and results over background soil, Atmos. Environ., 32, 873–882, 1998.

Choi, H. D. and Holsen, T. M. Gaseous mercury emissions from unsterilized and sterilized soils: the effect of temperature and UV radiation, Environ. Pollut., 157, 1673–1678, 2009.

Ci, Z. J., Zhang, X. S., Wang, Z. W., and Niu, Z. C.: Phase speciation of mercury (Hg) in coastal water of the Yellow Sea, China, Mar. Chem., 126, 250–255, 2011.

Ci, Z. J., Zhang, X. S., and Wang, Z. W.: Enhancing atmospheric mercury research in China to improve the current understanding of the global mercury cycle: the need for urgent and closely coordinated efforts, Environ. Sci. Technol., 46, 5636–5642, 2012.

Ci, Z. J., Zhang, X. S., Yin, Y. G., Chen, J. S., and Wang, S. W.: Mercury redox chemistry in waters of the eastern Asian seas: from polluted coast to clean open ocean, Environ. Sci. Technol., 50, 2371–2380, 2016a.

Ci, Z. J., Zhang, X. S., and Wang, Z. W.: Air–sea exchange of gaseous mercury in the tropical coast (Luhuitou fringing reef) of the South China Sea, the Hainan Island, China, Environ. Sci. Pollut. Res., 23, 11323–11329, 2016b.

Cobbett, F. D., Steffen, A., Lawson, G., and Van Heyst, B. J.: GEM fluxes and atmospheric mercury concentrations (GEM, RGM and Hgp) in the Canadian Arctic at Alert, Nunavut, Canada (February–June 2005), Atmos. Environ., 41, 6527–6543, 2007.

Corbett-Hains, H., Walters, N. E., and Van Heyst, B. J.: Evaluating the effects of sub-zero temperature cycling on mercury flux from soils, Atmos. Environ., 63, 102–108, 2012.

Dommergue, A., Ferrari, C. P., Poissant, L., Gauchard, P. A., and Boutron, C. F.: Diurnal cycles of gaseous mercury within the snowpack at Kuujjuarapik/Whapmagoostui, Quebec, Canada, Environ. Sci. Technol., 37, 3289–3297, 2003.

Dommergue, A., Bahlmann, E., Ebinghaus, R., Ferrari, C., and Boutron, C.: Laboratory simulation of Hg^0 emissions from a snowpack, Anal. Bioanal. Chem., 388, 319–327, 2007.

Dommergue, A., Barret, M., Courteaud, J., Cristofanelli, P., Ferrari, C. P., and Gallée, H.: Dynamic recycling of gaseous elemental mercury in the boundary layer of the Antarctic Plateau, Atmos. Chem. Phys., 12, 11027–11036, doi:10.5194/acp-12-11027-2012, 2012.

Durnford, D. A. and Dastoor, A.: The behavior of mercury in the cryosphere: A review of what we know from observations, J. Geophys. Res., 116, D06305, doi:10.1029/2010JD014809 2011.

Durnford, D. A., Dastoor, A. P., Steen, A. O., Berg, T., Ryzhkov, A., Figueras-Nieto, D., Hole, L. R., Pfaffhuber, K. A., and Hung, H.: How relevant is the deposition of mercury onto snowpacks? – Part 1: A statistical study on the impact of environmental factors, Atmos. Chem. Phys., 12, 9221–9249, doi:10.5194/acp-12-9221-2012, 2012a.

Durnford, D. A., Dastoor, A., Ryzhkov, A., Poissant, L., Pilote, M., and Figueras-Nieto, D.: How relevant is the deposition of mercury onto snowpacks? – Part 2: A modeling study, Atmos. Chem. Phys., 12, 9251–9274, doi:10.5194/acp-12-9251-2012, 2012b.

Ebinghaus, R., Jennings, S. G., Kock, H. H., Derwent, R. G., Manning, A. J., and Spain, T. G.: Decreasing trends in total gaseous mercury observations in baseline air at Mace Head, Ireland from 1996 to 2009, Atmos. Environ., 45, 3475–3480, 2011.

Eckley, C. S., Gustin, M., Lin, C-J., Li, X., and Miller, M. B.: The influence of dynamic chamber design and operating parameters on calculated surface–to–air mercury fluxes, Atmos. Environ., 44, 194–203, 2010.

Eckley, C. S., Gustin, M., Marsik, F., and Miller, M. B.: Measurement of surface mercury fluxes at active industrial gold mines in Nevada (USA), Sci. Total Environ., 409, 514–522, 2011.

Edwards, G. C., and Howard, D. A. Air–surface exchange measurements of gaseous elemental mercury over naturally enriched and background terrestrial landscapes in Australia, Atmos. Chem. Phys., 13, 5325–5336, doi:10.5194/acp-13-5325-2013, 2013.

Engle, M. A., Gustin, M. S., Lindberg, S. E., and Gerler, A. W.: Investigation of the effect of tropospheric oxidants on Hg emissions from substrates, Mater. Geoenviron., 51, 1546–1549, 2004.

Ericksen, J. A., Gustin, M. S., Lindberg, S. E., Olund, S. D., and Krabbenhoft, D. P.: Assessing the potential for re-emission of mercury deposited in precipitation from arid soils using a stable isotope, Environ. Sci. Technol., 39, 8001–8007, 2005.

Ericksen, J. A., Gustin, M. S., Xin, M., Weisberg, P. J., and Fernandez, G. C. J.: Air–soil exchange of mercury from background soils in the United States, Sci. Total Environ., 366, 851–863, 2006.

Faïn, X., Grangeon, S., Bahlmann, E., Fritsche, J., Obrist, D., Dommergue, A., Ferrari, C. P., Cairns, W., Ebinghaus, R., and Barbante, C.: Diurnal production of gaseous mercury in the alpine snowpack before snowmelt, J. Geophys. Res. Atmos., 112, 5671–5674, 2007.

Ferrari, C. P., Gauchard, P., Aspmo, K., Dommergue, A., Magand, O., Bahlmann, E., Nagorski, S., Temme, C., Ebinghaus, R., Steffen, A., Banic, C., Berg, T., Planchon, F., Barbante, C., Cescon, P., and Boutron, C. F.: Snow–to–air exchanges of mercury in an Arctic seasonal snow pack in Ny-Ålesund, Svalbard, Atmos. Environ., 39, 7633–7645, 2005.

Fitzgerald, W. F. and Gill, G. A.: Subnanogram determination of mercury by two-stage gold amalgamation and gas phase detection applied to atmospheric analysis, Anal. Chem., 51, 1714–1720, 1979.

Fu, X. W., Feng, X. B., and Wang, S. F.: Exchange fluxes of Hg between surfaces and atmosphere in the eastern flank of Mount Gongga, Sichuan province, southwestern China, J. Geophys. Res. Atmos., 113, D20, doi:10.1029/2008JD009814, 2008a.

Fu, X. W., Feng, X. B., Zhu, W. Z., Wang, S. F., and Lu, J.: Total gaseous mercury concentrations in ambient air in the eastern slope of Mt. Gongga, South-Eastern fringe of the Tibetan plateau, China, Atmos. Environ., 42, 970–979, 2008b.

Fu, X. W., Feng, X., Liang, P., Deliger, Zhang, H., Ji, J., and Liu, P.: Temporal trend and sources of speciated atmospheric mercury at Waliguan GAW station, northwestern China, Atmos. Chem. Phys., 12, 1951–1964, doi:10.5194/acp-12-1951-2012, 2012.

Gabriel, M. C. and Williamson, D. G.: Some insight into the influence of urban ground surface properties on the air–surface exchange of total gaseous mercury, Appl. Geochem., 23, 794–806, 2008.

Gabriel, M. C., Williamson, D. G., Zhang, H., Brooks, S., and Lindberg, S.: Diurnal and seasonal trends in total gaseous mercury flux from three urban ground surfaces, Atmos. Environ., 40, 4269–4284, 2006.

Gabriel, M. C., Williamson, D. G., and Brooks, S.: Potential impact of rainfall on the air–surface exchange of total gaseous mercury from two common urban ground surfaces, Atmos. Environ., 45, 1766–1774, 2011.

Gustin, M. S. and Stamenkovic, J.: Effect of watering and soil moisture on mercury emissions from soils, Biogeochemistry, 76, 215–232, 2005.

Gustin, M. S., Taylor Jr, G. E., and Maxey, R. A.: Effect of temperature and air movement on the flux of elemental mercury from substrate to the atmosphere, J. Geophys. Res. Atmos., 102, 3891–3898, 1997.

Gustin, M. S., Lindberg, S., Marsik, F., Casimir, A., Ebinghaus, R., Edwards, G., Hubble-Fitzgerald, C., Kemp, R., Kock, H., Leonard, T., London J., Majewski, M., Montecinos, C., Owens, J., Pilote, M., Poissant, L., Rasmussen, P., Schaedlich, F., Schneeberger, D., Schroeder, W., Sommar, J., Turner, R., Vette, A., Wallschlaeger, D., Xiao, Z., and Zhang, H.: Nevada STORMS project: Measurement of mercury emissions from naturally enriched surfaces, J. Geophys. Res. Atmos., 104, D17, 21831–21844, 1999.

Gustin, M. S., Biester, H., and Kim, C. S.: Investigation of the light-enhanced emission of mercury from naturally enriched substrates, Atmos. Environ., 36, 3241–3254, 2002.

Gustin, M. S., Ericksen, J. A., Schorran, D. E., Johnson, D. W., Lindberg, S. E., and Coleman, J. S.: Application of controlled mesocosms for understanding mercury air–soil–plant exchange, Environ. Sci. Technol., 38, 6044–6050, 2004.

Gustin, M. S., Engle, M., Ericksen, J., Lyman, S., Stamenkovic, J., and Xin, M.: Mercury exchange between the atmosphere and low mercury containing substrates, Appl. Geochem., 21, 1913–1923, 2006.

Hintelmann, H., Harris, R., Heyes, A., Hurley, J. P., Kelly, C. A., Krabbenhoft, D. P., Lindberg, S., Rudd, J. W. M., Scott, K. J., and Louis, V. L. S.: Reactivity and mobility of new and old mercury deposition in a boreal forest ecosystem during the first year of the METAALICUS study, Environ. Sci. Technol., 36, 5034–5040, 2002.

Huang, J., Kang, S. C., Zhang, Q. G., Jenkins, M. G., Guo, J. M., Zhang, G. S., and Wang, K.: Spatial distribution and magnification processes of mercury in snow from high-elevation glaciers in the Tibetan Plateau, Atmos. Environ., 46, 140–146, 2012.

Huang, J., Kang, S. C., Wang, S. X., Wang, L., Zhang, Q. G., Guo, J. M., Wang, K., Zhang, G. S., and Tripathee, L.: Wet deposition of mercury at Lhasa, the capital city of Tibet, Sci. Total Environ., 447, 123–132, 2013.

Jiskra, M., Wiederhold, J. G., Skyllberg, U., Kronberg, R. M., Hajdas, I., and Kretzschmar, R.: Mercury deposition and re-emission pathways in boreal forest soils investigated with Hg isotope signatures, Environ. Sci. Technol., 49, 7188–7196, 2015.

Johnson, D. W., Benesch, J. A., Gustin, M. S., Schorran, D. S., Lindberg, S. E., and Coleman, J. S.: Experimental evidence against diffusion control of Hg evasion from soils, Sci. Total Environ., 304, 175–184, 2003.

Kang, S. C., Xu, Y. W., You, Q. L., Flügel, W., Pepin, N., and Yao, T. D.: Review of climate and cryospheric change in the Tibetan Plateau, Environ. Res. Lett., 5, 015101, doi:10.1088/1748-9326/5/1/015101, 2010.

Khwaja, A. R., Bloom, P. R., and Brezonik, P. L.: Binding constants of divalent mercury (Hg^{2+}) in soil humic acids and soil organic matter, Environ. Sci. Technol., 40, 844–849, 2006.

Kim, K. H. and Lindberg, S. E.: Design and initial tests of a dynamic enclosure chamber for measurements of vapor-phase mercury fluxes over soils, Water Air Soil Pollut., 80, 1059–1068, 1995.

Klusman, R. W. and Webster, J. D.: Meteorological noise in crustal gas emission and relevance to geochemical exploration, J. Geochem. Explor., 15, 63–76, 1981.

Kocman, D. and Horvat, M.: A laboratory based experimental study of mercury emission from contaminated soils in the River Idrijca catchment, Atmos. Chem. Phys., 10, 1417–1426, doi:10.5194/acp-10-1417-2010, 2010.

Krabbenhoft, D. P. and Sunderland, E. M.: Global change and mercury, Science, 341, 1457–1458, 2013.

Lalonde, J. D., Poulain, A. J., and Marc, A.: The role of mercury redox reactions in snow on snow–to–air mercury transfer, Environ. Sci. Technol., 36, 174–178, 2001.

Lalonde, J. D., Amyot, M., Doyon, M., and Auclair, J.: Photo-induced Hg(II) reduction in snow from the remote and temperate Experimental Lakes Area (Ontario, Canada), J. Geophys. Res. Atmos., 108, 471–475, 2003.

Lin, C. J., Gustin, M. S., Singhasuk, P., Eckley, C., and Miller, M.: Empirical models for estimating mercury flux from soils, Environ. Sci. Technol., 44, 8522–8528, 2010.

Lindberg, S. E., Zhang, H., Gustin, M., Vette, A., Marsik, F., Owens, J., Casimir, A., Ebinghaus, R., Edwards, G., Fitzgerald, C., Kemp, J., Kock, H. H., London, J., Majewski, M., Poissant, L., Pilote, M., Rasmussen, P., Schaedlich, F., Schneeberger, D., Sommar, J., Turner, R., Wallschläger, D., and Xiao, Z.: Increases in mercury emissions from desert soils in response to rainfall and irrigation, J. Geophys. Res. Atmos., 104, 21879–21888, 1999.

Loewen, M., Kang, S. C., Armstrong, D., Zhang, Q. G., Tomy, G., and Wang, F. Y.: Atmospheric transport of mercury to the Tibetan Plateau, Environ. Sci. Technol., 41, 7632–7638, 2007.

Malcolm, E. G. and Keeler, G. J.: Measurements of mercury in dew: atmospheric removal of mercury species to a wetted surface, Environ. Sci. Technol., 36, 2815–2821, 2002.

Mann, E., Ziegler, S., Mallory, M., and O'Driscoll, N.: Mercury photochemistry in snow and implications for Arctic ecosystems, Environ. Rev., 22, 331–345, 2014.

Mann, E. A., Mallory, M. L., Ziegler, S. E., Tordon, R., and O'Driscoll, N. J.: Mercury in Arctic snow: quantifying the kinetics of photochemical oxidation and reduction, Sci. Total Environ., 509/510, 115–132, 2015.

Mauclair, C., Layshock, J., and Carpi, A.: Quantifying the effect of humic matter on the emission of mercury from artificial soil surfaces, Appl. Geochem., 23, 594–601, 2008.

Mazur, M. E. E., Eckley, C. S., and Mitchell, C. P. J.: Susceptibility of soil bound mercury to gaseous emission as a function of source depth: an enriched isotope tracer investigation, Environ. Sci. Technol., 49, 9143–9149, 2015.

Moore, C. and Carpi, A.: Mechanisms of the emission of mercury from soil: Role of UV radiation, J. Geophys. Res., 110, D24302, doi:10.1029/2004JD005567, 2005.

NSIDC: National Snow and Ice Data Center, USA, www.nsidc.org, 2016.

Park, S. Y., Holsen, T. M., Kim, P. R., and Han, Y. J.: Laboratory investigation of factors affecting mercury emissions from soils, Environ. Earth Sci., 72, 2711–2721, 2014.

Peng, F., Xue, X., You, Q., Zhou, X., and Wang, T.: Warming effects on carbon release in a permafrost area of Qinghai-Tibet Plateau, Environ. Earth Sci., 73, 57–66, 2015a.

Peng, F., Xu, M., You, Q., Zhou, X., Wang, T., and Xue, X.: Different responses of soil respiration and its components to experimental warming with contrasting soil water content, Arct. Antarct. Alp. Res., 47, 359–368, 2015b.

Pirrone, N. and Mason, R. P. (Eds.): Hg fate and transport in the global atmosphere: emissions, measurements and models, Springer, Geneva, 2009.

Poissant, L., Pilote, M., and Casimir, A.: Mercury flux measurements in a naturally enriched area: Correlation with environmental conditions during the Nevada Study and Tests of the Release of Mercury From Soils (STORMS), J. Geophys. Res., 104, 21845–21857, 1999.

Schlüter, K.: Review: evaporation of mercury from soils. An integration and synthesis of current knowledge, Environ. Geol., 39, 249–271, 2000.

Schuster, E.: The behavior of mercury in the soil with special emphasis on complexation and adsorption processes–a review of the literature, Water Air Soil Pollut., 56, 667–680, 1991.

Selin, N. E.: Global biogeochemical cycling of mercury: A review, Annu. Rev. Env. Resour., 34, 43–63, 2009.

Sommar, J., Zhu, W., Lin, C. J., and Feng, X.: Field approaches to measure mercury exchange between natural surfaces and the atmosphere – a review, Crit. Rev. Environ. Sci. Technol., 43, 1657–1739, 2013.

Song, X. and Van Heyst, B.: Volatilization of mercury from soils in response to simulated precipitation, Atmos. Environ., 39, 7494–7505, 2005.

Sprovieri, F., Pirrone, N., Ebinghaus, R., Kock, H., and Dommergue, A.: A review of worldwide atmospheric mercury measurements, Atmos. Chem. Phys., 10, 8245–8265, doi:10.5194/acp-10-8245-2010, 2010.

Steen, A. O., Berg, T., Dastoor, A. P., Durnford, D. A., Hole, L. R., and Pfaffhuber, K. A.: Dynamic exchange of gaseous elemental mercury during polar night and day, Atmos. Environ., 43, 5604–561, 2009.

Streets, D. G., Hao, J., Wu, Y., Jiang, J., Chan, M., Tian, H., and Feng, X.: Anthropogenic mercury emissions in China, Atmos. Environ., 39, 7789–7806, 2005.

Toyota, K., McConnell, J. C., Staebler, R. M., and Dastoor, A. P.: Air–snowpack exchange of bromine, ozone and mercury in the springtime Arctic simulated by the 1-D model PHANTAS – Part 1: In-snow bromine activation and its impact on ozone, Atmos. Chem. Phys., 14, 4101–4133, doi:10.5194/acp-14-4101-2014, 2014a.

Toyota, K., Dastoor, A. P., and Ryzhkov, A.: Air–snowpack exchange of bromine, ozone and mercury in the springtime Arctic simulated by the 1-D model PHANTAS – Part 2: Mercury and its speciation, Atmos. Chem. Phys., 14, 4135–4167, doi:10.5194/acp-14-4135-2014, 2014b.

Wang, D. Y., He, L., Shi, X. J., Wei, S. Q., and Feng, X. B.: Release flux of mercury from different environmental surfaces in Chongqing, China, Chemosphere, 64, 1845–1854, 2006.

Wang, S. F., Feng, X. B., Qiu, G. L., Shang, L. H., Li, P., and Wei, Z. Q.: Mercury concentrations and air/soil fluxes in Wuchuan mercury mining district, Guizhou province, China, Atmos. Environ., 41, 5984–5993, 2007.

Wang, X. P., Yao, T. D., Wang, P. L., and Tian, L. D.: The recent deposition of persistent organic pollutants and mercury to the Dasuopu glacier, Mt. Xixiabangma, central Himalayas, Sci. Total Environ., 394, 134–143, 2008.

Wei, K., Chen, W., and Huang, R. H.: Long-term changes of the ultraviolet radiation in China and its relationship with total ozone and precipitation, Adv. Atmos. Sci., 23, 700–710, 2006.

Xin, M. and Gustin, M. S.: Gaseous elemental mercury exchange with low mercury containing soils: Investigation of controlling factors, Appl. Geochem., 22, 1451–1466, 2007.

Xin, M., Gustin, M., and Johnson, D.: Laboratory investigation of the potential for re-emission of atmospherically derived Hg from soils, Environ. Sci. Technol., 41, 4946–4951, 2007.

Yang, Y. K., Zhang, C., Shi, X. J., Lin, T., and Wang, D. Y.: Effect of organic matter and pH on mercury release from soils, J. Environ. Sci., 19, 1349–1354, 2007.

Yin, X. F., Zhang Q. G., Tong Y. D., Zhang W., Wang X. J., Schauer J., and Kang S. C.: Observations of atmospheric mercury at a high altitude site in the Tibetan plateau in the winter of 2014/2015: concentrations, speciation and insight into atmospheric hg in free troposphere, 12th International Conference on Mercury as a Global Pollutant, 14–19 June, Jeju, Korea, 2015.

Zhang, H. and Lindberg, S. E.: Processes influencing the emission of mercury from soils: A conceptual model, J. Geophys. Res. Atmos., 104, 21889–21896, 1999.

Zhang, Q. G., Huang, J., Wang, F. Y., Mark, L., Xu, J. Z., Armstrong, D., Li, C. L., Zhang, Y. L., and Kang, S. C.: Mercury distribution and deposition in glacier snow over western China, Environ. Sci. Technol., 46, 5404–5413, 2012.

Zhou, L., Zou, H., Shupo, M. A., and Peng, L. I.: The Tibetan ozone low and its long-term variation during 1979–2010, Acta Meteorol. Sin., 27, 75–86, 2013.

Zhu, J. S., Wang, D. Y., Liu, X., and Zhang, Y. T.: Mercury fluxes from air/surface interfaces in paddy field and dry land, Appl. Geochem., 26, 249–255, 2011.

Zhu, W., Lin, C.-J., Wang, X., Sommar, J., Fu, X., and Feng, X.: Global observations and modeling of atmosphere–surface exchange of elemental mercury: a critical review, Atmos. Chem. Phys., 16, 4451–4480, doi:10.5194/acp-16-4451-2016, 2016.